

Spin-glass state in CuGa₂O₄

G.A. Petrakovskii, K.S. Aleksandrov, L.N. Bezmaternikh, S.S. Aplesnin
Institute of Physics, Academy of Sciences, Siberian Branch, 660036 Krasnoyarsk, Russia

B. Roessli, F. Semadeni

Laboratory for Neutron Scattering, Paul Scherrer Institute and ETH Zurich, CH-5232 Villigen PSI, Switzerland

A. Amato, C. Baines

Laboratory for Muon-Spin Spectroscopy, Paul Scherrer Institute, CH-5232 Villigen PSI, Switzerland

J. Bartolomé, M. Evangelisti*

Instituto de Ciencia de Materiales de Aragón, CSIC-Universidad de Zaragoza, Ciudad Universitaria, 50009 Zaragoza, Spain
 (October 26, 2018)

Magnetic susceptibility, magnetization, specific heat and positive muon spin relaxation (μ SR) measurements have been used to characterize the magnetic ground-state of the spinel compound CuGa₂O₄. We observe a spin-glass transition of the S=1/2 Cu²⁺ spins below T_f = 2.5K characterized by a cusp in the susceptibility curve which is suppressed when a magnetic field is applied. We show that the magnetization of CuGa₂O₄ depends on the magnetic history of the sample. Well below T_f, the muon signal resembles the dynamical Kubo-Toyabe expression reflecting that the spin freezing process in CuGa₂O₄ results in a Gaussian distribution of the magnetic moments. By means of Monte-Carlo simulations, we obtain the relevant exchange integrals between the Cu²⁺ spins in this compound.

75.50.L, 76.75, 75.40.Cx, 02.70.Lq

I. INTRODUCTION

Although spin glasses have been extensively studied in the past years, there is still no consensus about the ground-state and dynamics in these systems (for an introduction see e.g. K.H. Fisher and J.A. Hertz [1]). It is generally accepted that both site-disorder and competition between the magnetic moments are necessary to produce a low-temperature state where the spins are frozen along arbitrary directions². Examples of such systems are metallic spin-glasses where magnetic impurities are randomly diluted in a noble metal³. For this particular class of materials competition between the magnetic moments is the result of the Rudermann-Kittel-Kasuya-Yosida (RKKY) interaction⁴ where ferromagnetic and antiferromagnetic exchange interactions alternate as a function of distance between neighboring spins. The RKKY interaction cannot be invoked for localized magnets and the spin-glass transition in these systems must be realized by other mechanisms. Typical insulating spin-glasses of this kind are the alloys Eu_xSr_{1-x}S. In the x=0-limit, EuS is a well-known example of an isotropic 3-dimensional Heisenberg ferromagnet. The exchange integrals have been determined by inelastic neutron scattering in this material with the result that ferromagnetic nearest-neighbor exchange interaction competes with next-nearest antiferromagnetic coupling⁵. Diluting non-magnetic Sr for Eu ensures bond-randomness and the conditions for obtaining a spin-glass state are fulfilled in a large range of impurity concentrations⁶, in

qualitative agreement with the molecular-field theory of Edwards and Anderson⁷. De Seze pointed out that a spin-glass phase transition can occur in a geometrically frustrated system with Ising spins and antiferromagnetic interactions only⁸. Following De Seze's work, Villain⁹ proposed that spin glasses can be obtained in materials with geometric frustration and Heisenberg-type exchange interactions like cubic spinels. These compounds have the chemical formula AB₂O₄. The chemical structure of spinels consists of both tetrahedral and octahedral sites. The number of crystallographic sites is larger than the number of A and B cations in the chemical formula, so that the cations generally distribute randomly among the available atomic positions. In particular, this random distribution of cations determines in a large extent the microwave relaxation properties of the spinel compounds¹⁰. When both sublattices are occupied by magnetic ions the ground state is a ferrimagnet. The B sublattice builds connected tetrahedra and antiferromagnetic interactions induce topological frustrations¹¹ which can lead to a spin-glass state when non-magnetic impurities are introduced¹⁹. The dominant magnetic interaction in most of these materials is antiferromagnetic and connects spins between the A and B sublattices while the A-A and B-B exchange interactions are comparatively small. However, intersublattice exchange constants can modify the magnetic phase diagram originally calculated by Villain and for real systems the situation is usually complicated¹². Although spin-glass transition has been found in diluted spinels¹³, spin-glass transition in pure

cubic spinels is less common.

In this article, we report magnetic susceptibility, magnetization measurements in fields up to 50 KOe, specific heat and muon-spin relaxation (μ SR) measurements in the cubic spinel CuGa_2O_4 . The results show that CuGa_2O_4 undergoes a paramagnetic to spin-glass phase-transition at $T_f = 2.5\text{K}$. By means of Monte-Carlo simulations, the relevant exchange interactions are obtained for CuGa_2O_4 . We show that the formation of a spin-glass ground-state in CuGa_2O_4 is due to the Jahn-Teller character of the Cu^{2+} ions. Specifically, in a field of octahedral symmetry, the Jahn-Teller effect distorts the electronic d levels of the Cu^{2+} which become split by the effect of the crystal field into a threefold degenerate level and a twofold degenerate one. In such compounds there is an interaction between the electronic system with the underlying lattice which very often leads to a structural phase transition. Typical compounds exhibiting cooperative Jahn-Teller distortion are found in *e.g.* perovskites (KCuF_3 , LaMnO_3), spinels (CuFe_2O_4 , Mn_3O_4), rutiles (CrF_2 , CuF_2) or garnets ($\text{Ca}_3\text{Fe}_2\text{Ge}_3\text{O}_{12}$). The structural phase transition can be accompanied by orbital-ordering of the d -electrons which in turn influences the nature of the exchange interaction. The important role of the Jahn-Teller effect in forming the magnetic ground-state in the perovskite manganites which exhibit colossal magnetoresistance (*e.g.* see [14] and references therein) and in cuprates (*e.g.* [15,16] and references therein) is currently a subject of intense investigation both theoretically and experimentally. In that respect, we note that the influence of the Jahn-Teller effect on the properties of the magnetic insulators is discussed in detail by Kugel and Khomsky¹⁷.

II. EXPERIMENTAL DETAILS

A. Sample Preparation

Single crystals of CuGa_2O_4 were grown by spontaneous crystallization starting from a $\text{CuO}-\text{Ga}_2\text{O}_3$ solution melt in $\text{PbO}-0.64\text{B}_2\text{O}_3-0.5\text{Na}_2\text{O}$. After slowly cooling the melt to room temperature, single crystals of typical size $3 \times 3 \times 3 \text{ mm}^3$ and of octahedral shape were obtained. X-Ray diffraction analysis showed that the CuGa_2O_4 crystals used for the present experiments are cubic spinels with both copper and gallium ions randomly distributed in the A and B sublattices in agreement with previous diffraction investigation (see Ref. [18]). The chemical structure of CuGa_2O_4 is described by the space-group $Fd\bar{3}m$ with lattice constants $a=8.39\text{\AA}$ at room temperature.

B. Magnetic Measurements

The magnetic susceptibility and magnetization measurements were performed with a commercial MPMS Quantum Design SQUID magnetometer together with an AC-susceptibility option at ICMA, Spain. The amplitude of the AC-magnetic field was set to 4.5 Oe with the frequency of the field being varied between 0.1 Hz and 990 Hz. The measurements were carried out in the temperature range 1.7-300 K and in applied magnetic fields up to 50 kOe. Additional measurements of the magnetic susceptibility in the temperature range $T=4.2\text{K}$ to 120K were performed at the Institute of Physics, Krasnoyarsk, using a home-built SQUID magnetometer.

C. Specific Heat Measurements

The specific heat measurements were performed with a commercial PPMS device (Quantum Design) in the temperature range $1.8 \text{ K} \leq T \leq 10 \text{ K}$. We used a small single crystal of mass $\sim 4.15\text{mg}$. The raw data were corrected for the copper host and glue, which were measured separately. We did not attempt to subtract the phonon contribution, as it is expected to be small at low temperatures.

D. Muon-Spin Relaxation

The μ SR experiments were performed on the LTF spectrometer at the Paul-Scherrer Institute, Switzerland. The data were recorded using the zero-field method which is very sensitive to determine both static and dynamic effects in spin-glasses²³. Additional measurements were performed as a function of applied magnetic field. In that case, the sample was zero-field cooled. The sample we used for the present experiment consists of about 50 pieces of the above described crystals which were glued on a silver plate. The sample was enclosed in a top-loading $^3\text{He}-^4\text{He}$ dilution cryostat and the measurements were carried out in the temperature range $650 \text{ mK} \leq T \leq 10 \text{ K}$.

III. MAGNETIZATION, SUSCEPTIBILITY AND SPECIFIC HEAT RESULTS

Figure1 shows the result of the magnetic susceptibility measurements with an AC-frequency of 19 Hz and an excitation amplitude of $H=4.5 \text{ Oe}$. For temperatures higher than $T=20 \text{ K}$, the magnetic susceptibility is well reproduced by the Curie-Weiss law. Upon lowering the temperature below $T=20 \text{ K}$, the magnetic susceptibility increases continuously. The real part of the magnetic susceptibility shows a cusp at $T_f \simeq 2.5\text{K}$ which is independent of the relative orientation of the magnetic field

with respect to the crystal axes. The imaginary part of the magnetic susceptibility also exhibits a maximum at the same temperature. To understand the nature of the maxima appearing in the susceptibility curves, the magnetization in CuGa_2O_4 was determined as a function of applied magnetic field and for different magnetic histories of the samples. As an example, Fig. 2 shows the magnetization curves obtained in CuGa_2O_4 after zero-field and field-cooling, respectively. For the latter case, the sample was cooled in a magnetic field of $H=100$ Oe applied along the [001] crystal axis. It is evident from the figure that for temperatures below $T_f \simeq 2.5$ K the magnetization shows a temperature hysteresis, which is an usual characteristic for the formation of a spin-glass state. The results of the magnetic susceptibility measurements taken for different magnetic fields are presented in Fig. 3 which shows that magnetic fields larger than $H=5$ kOe suppress the cusp observed at T_f in zero-magnetic field. Figure 4 shows that the increase of the magnetic moment as a function of magnetic field is far from saturation at the maximum field of 5T. In Fig. 5 the temperature dependence of the transition temperature T_f of the spin-glass transition is observed to increase as a function of increasing AC-frequency. The above experimental results all indicate that the Cu^{2+} magnetic moments in CuGa_2O_4 undergo a phase transition to a spin-glass ground state below $T_f \simeq 2.5$ K. This is also confirmed by the calorimetric measurements performed in zero-magnetic field for this compound. A plot of the specific heat C_p/T in CuGa_2O_4 is shown in Fig. 6. The data do not show any indication of a phase transition to a 3-dimensional ferro- or antiferro-magnetic ordered state. However, a broad maximum is observed around $T = 2.5$ K followed by a slow decay toward high temperatures. This particular behavior of the specific heat as a function of temperature is reminiscent of a spin-glass transition¹⁹.

IV. DISCUSSION OF THE BULK MEASUREMENTS

A spin-glass state is characterized by an assembly of magnetic moments which are frozen along random and arbitrary directions in space below a specific transition temperature T_f . Because of the non-ergodicity of the system, the phenomenon is irreversible. The macroscopic magnetization of a spin-glass system is equal to zero in the absence of a magnetic field. On the other hand, cooling a spin-glass in an external magnetic field transfers the system into a metastable state with a non-zero magnetization value. For temperatures above the spin-freezing temperature T_f , the magnetic moments are in a paramagnetic state and consequently the temperature dependence of the magnetic susceptibility follows the Curie-Weiss law

$$\chi(T) = \frac{C}{T - \theta}, \quad (1)$$

where $C = Ng^2\mu_B^2S(S+1)/3k_B$ is the Curie constant and θ the paramagnetic Curie temperature. N is the magnetic moment density, g the Landé factor and μ_B the Bohr magneton. S corresponds to the spin value of Cu^{2+} and k_B is the Boltzmann constant. From the magnetic susceptibility measurements presented above, we obtain for CuGa_2O_4 the values $1/C=0.34$ emu K/mol, $\theta = -8$ and $\mu_{\text{eff}} = g\sqrt{S(S+1)}\mu_B = 1.65\mu_B$. The magnetic susceptibility is related to the Edwards-Anderson (EA) parameter⁷ $q = \lim_{t \rightarrow \infty} [\langle S_i(t)S_i(0) \rangle]_{\text{av}}$ through the relation

$$\chi(T) = C \frac{1 - q(T)}{T - \theta(1 - q(T))}. \quad (2)$$

According to the percolation theory of Kirkpatrick²⁰, the EA-parameter follows a power law $q(T) \propto (1 - T/T_f)^\beta$ close to the spin-glass temperature T_f with β equal to 0.39. However, near T_f , we found the value $\beta = 0.16$ in CuGa_2O_4 . The frequency dependence of the spin freezing temperature T_f is a characteristic feature of the spin-glass state. It has been experimentally found that in spin-glasses T_f decreases with increasing AC-frequency. A quantitative measure of the frequency shift is obtained from $(\Delta T_f/T_f)/\Delta \log(\omega) = 0.067$. This is very similar to other insulating spin-glasses such as (EuSr)S or (FeMg)Cl₂ [21] and one order of magnitude lower than in canonical metallic spin glasses, or one order of magnitude larger than in a superparamagnet. The magnetic field and temperature dependence of the magnetization $M(H,T)$ for a spin-glass system with Heisenberg spins of dimension m has been calculated by Toulouse and Gabau²². Within the Sherrington-Kirkpatrick (SK) model and for temperatures below T_f , the expression for the magnetization is accordingly given by

$$M/H = 1 - [4/(m+2)]^{1/3} 3h^{4/3}/4 \quad (3)$$

where $h = g\mu_B H/k_B T_f$ is the reduced magnetic field. Figure 7 shows a comparison between the experimental measurements obtained in CuGa_2O_4 and Eq.3. There is a good agreement between theory and experiment for reduced magnetic fields below $h = 0.6$. For larger values of the reduced magnetic field h , however, there is a significant discrepancy between the observed and calculated values of the magnetization, which can be attributed to the fact that the SK theory is based on the mean-field approximation and makes use of infinite long-range interactions between the spins. On the contrary, the magnetic exchange interactions in CuGa_2O_4 have short-range character. Moreover, the domain of validity of the mean-field theory for a spin-1/2 compound is unclear, in particular close to the transition temperature T_f where the critical fluctuations become important. In the same spirit, the freezing temperature T_f shows a much more pronounced magnetic-field dependence than predicted by mean-field theory

$$h^{2/3} = [4/(m+2)]^{1/3} (1 - T_f(H)/T_f(0)), \quad (4)$$

as evidenced in Fig.8.

V. μ SR RESULTS

To get more insight into both the static and dynamic properties of the Cu^{2+} magnetic moments in CuGa_2O_4 , we have measured the muon-spin relaxation above and below the freezing temperature T_f in this material. Generally, the magnetic interactions probed by the implanted spin-polarized muon are detected by monitoring the asymmetric emission of positrons arising from the weak decay of the muon. Recording the positron rate $N(t)$ as a function of muon life-time yields

$$N(t) = N(0) \exp(-t/\tau)[1 + AG_z(t)] , \quad (5)$$

where A is the initial muon asymmetry parameter. The product $AG_z(t)$ is often called the μ SR signal. In addition, the function $G_z(t)$ can be associated with the muon spin auto-correlation function, i.e.

$$G_z(t) = \frac{\langle \mathbf{S}(t)\mathbf{S}(0) \rangle}{S^2(0)} , \quad (6)$$

where \mathbf{S} is the spin of the muon. Typical zero-field μ SR signals measured in CuGa_2O_4 are shown in Fig. 9. Above $T \simeq 3.8$ K (and at least up to 10 K), the data are best described by assuming for $G_z(t)$ the form

$$G_{z,para}(t) = G_{KT}(t) \cdot G_{es}(t) , \quad (7)$$

with G_{KT} representing the familiar Kubo-Toyabe (KT) expression²⁶

$$G_{KT}(t) = \frac{1}{3} + \frac{2}{3}(1 - \Delta_{ns}^2 t^2) \exp(-\frac{1}{2}\Delta_{ns}^2 t^2) , \quad (8)$$

and with G_{es} given by

$$G_{es}(t) = \exp[-(\lambda t)^\beta] . \quad (9)$$

The form of $G_{z,para}(t)$ points for the occurrence of two independent channels of depolarization acting on the muon spin. The first channel, giving rise to the KT function G_{KT} , originates from the nuclear dipole moments (Ga and Cu isotopes). The internal fields of this contribution are assumed to be Gaussian distributed in their values, randomly oriented and static within the μ SR time window. The parameter $\Delta_{ns}^2/\gamma_\mu^2$ represents the second moment of this field distribution due to the nuclear spins along one Cartesian axis ($\gamma_\mu = 2\pi \cdot 13.553879$ kHz/G is the gyro-magnetic ratio of the muon). The second channel, described by the function $G_{es}(t)$, which will be discussed in details below, represents the contribution arising from the fluctuating electronic Cu spins.

At $T = 10$ K the muon depolarisation can be satisfactorily described by assuming $G_{es}(t) = 1$, i.e. $G_{z,para}(t) = G_{KT}(t)$ with $\Delta_{ns} = 0.16(1)$ MHz (see also Fig. 9), indicating that the fluctuations of the electronic spins are still too fast to be observed in the μ SR time window. However, upon cooling the sample below $T = 10$ K and down

to 3.8 K, the fluctuation rate of the electronic spins decreases and the muon-spin depolarisation becomes gradually dominated by the $G_{es}(t)$ contribution. Figure 10 represents the temperature evolution of the depolarisation rate λ . Whereas the exponent β remains constant in this temperature interval (i.e. $\beta \simeq 0.78$), the depolarisation rate exhibits a marked critical-like divergence, which must be taken as a clear evidence of the approach to a magnetic phase transition as the temperature is decreased. This critical behavior at $T \simeq 2.5$ K indeed corresponds to the temperature of the cusp in the magnetic susceptibility and to the specific heat anomaly. It can therefore be associated to the occurrence of the spin-glass phase (see Figs. 1 and 6) in CuGa_2O_4 .

For spin-glass systems, the stretched exponential form for the electronic-spin contribution of the muon-spin depolarisation function $G_z(t)$ has been shown²⁴ to match the Kohlrausch-like stretched exponential for the local moments autocorrelation function itself, which in turn arises from a broad distribution of electronic-spin correlation times. In the particular case of moderately concentrated systems, the exponent β reaches the value of $\frac{1}{3}$ at T_f . On the other hand for conventional magnetic systems, the dynamic muon-spin depolarisation function assumes an exponential form (i.e. $\beta = 1$), reflecting the unique spin-relaxation frequency of the localized moments. The situation observed here for CuGa_2O_4 appears somewhat intermediate with an exponent β slightly, but definitively, below unity ($\simeq \frac{3}{4}$). This behavior is tentatively ascribed to the high concentration of local moments (Cu^{2+} ions), randomly distributed in different sublattices, for which a somewhat narrow distribution of electronic-spin correlation times could be expected.

In the temperature range between 3.8 and 10 K, the best fits with Eq. 7 provide a parameter Δ_{ns} for the KT function (i.e. essentially the width of the internal fields arising from the nuclear moments) which is practically constant, indicating that the nuclear moments remain static at all temperatures. This is also confirmed by measurements performed in applied longitudinal fields (LF). If the nuclear moments are static within the μ SR time window and if the applied field is sufficiently strong to quench the nuclear dipole field contribution (i.e. $G_{KT}(t) = 1$), the muon-spin depolarisation should arise solely from the dynamical electronic-spin contribution and the depolarisation function will assume the form $G_z(t) = G_{es}(t)$. This was indeed observed during LF measurements (see Fig. 11) for which a magnetic field of 0.02 T was sufficient to quench the nuclear dipolar moments. The muon depolarisation function is then well reproduced with the stretched exponential function described before, with parameters compatible with the ones extracted from the zero-field data.

For temperatures below $T = 3.8$ K, the muon depolarization increases significantly and assumes a Gaussian character at short times. For this temperature range, the best description of the data is obtained using the function

$$G_z(t) = A_{para}G_{z,para}(t) + A_{magn}G_{DKT}(t), \quad (10)$$

where $G_{z,para}(t)$ is defined above and $G_{DKT}(t)$ is the so-called dynamical Kubo-Toyabe (DKT) function²⁶, which reflects that the Gaussian internal field distribution due to the occurrence of static electronic-spins (second moment $\Delta_{es}^2/\gamma_\mu^2$) fluctuates at the rate ν . The first term of Eq. 10 is only present in the temperature interval between 3.8 and 2.5 K, i.e. in a region where paramagnetic domains appear to coexist with domains exhibiting static, albeit disordered, magnetic moments. Figure 12 shows the temperature evolution of the amplitude A_{magn} which mirrors the volume of the magnetic domains. Therefore, it appears that in CuGa₂O₄ the transition to a spin-glass state begins around $T \simeq 3.8$ K to form local clusters of frozen electronic spins which grow when the temperature is lowered and finally percolate at the same temperature where the specific anomaly is observed (i.e. $T \simeq 2.5$ K) and which can be therefore associated to T_f .

With the exception of some limiting cases, the DKT function cannot be expressed analytically and depends directly on the parameters ν and Δ_{es} . Figure 13 shows the temperature dependence of the parameter Δ_{es} which exhibits a clear increase below $\simeq 3.5$ K and can be associated to the temperature dependence of the static part of the electronic magnetic moments. The fluctuation rate ν was found to be constant below T_f ($\nu \simeq 3.7$ MHz). It is worthwhile to note that the DKT function, which appears to describe perfectly the data for $T \ll T_f$, assumes a single fluctuation rate ν for the internal fields sensed by the muon spin. This has to be connected to our simple picture that the slightly reduced value in the paramagnetic phase of the exponent β compared to unity must be related to a rather narrow distribution of electronic-spin correlation times. Interestingly, the DKT function describes the data more satisfactorily than the model of “coexisting static and dynamical fields” developed by Uemura *et al.*²⁷, and based on the theory of Edwards and Anderson⁷, where each local moment is taken as a vector sum of a static component and a dynamical component randomly fluctuating (see Fig.14). This indicates that in CuGa₂O₄, by decreasing the temperature, an increasing part of each Cu²⁺ moment become quasi-static (characterized by a slow fluctuation rate ν), whereas the remaining part does not affect the muon polarization due to fast fluctuations that are not accessible within the μ SR time window.

VI. MONTE-CARLO SIMULATIONS

The experimental observations presented in the preceding sections all indicate that the Cu²⁺ magnetic moments in CuGa₂O₄ undergo a phase transition to a spin-glass state at $T_f=2.5$ K. To understand the nature of this magnetic state, Monte-Carlo simulations were performed using a model of Heisenberg spins with compet-

ing exchange interactions including random anisotropies. These arise as the result of Jahn-Teller distortions of the octahedrons and tetrahedrons surrounding the Cu²⁺ positions¹⁷. The local distortions occur randomly along one of the three equivalent C₄ cubic axes. Consequently, the exchange interactions between nearest-neighbors spins located on tetrahedral (A-sites) and octahedral (B-sites) positions have tetragonal anisotropy. However, the direction of the tetragonal axis is random in a crystal with cubic symmetry. For the model calculations, we considered exchange interactions between nearest-neighbors Cu²⁺(A)–Cu²⁺(B) and second-nearest- neighbors Cu²⁺(B) – Cu²⁺(B) magnetic ions. We took into account the fact that in the spinel lattice the Cu²⁺ ions are randomly distributed between the A and B sites with occupation probabilities of 25% and 75%, respectively. Consequently, the model Hamiltonian for this spin system is given by

$$\mathbf{H} = - \sum_{\alpha=x,y,z} \sum_{i,j} J_{ij}^{\alpha\alpha} S_i^\alpha S_j^\alpha P_i^t P_j^0 - \sum_{i,j} K_{ij} S_i S_j P_i^t P_j^0 - \sum_i H S_i^z (P_i^t P_j^0), \quad (11)$$

where the $J_{ij}^{\alpha\alpha}$'s represent the exchange integrals between the nearest-neighbors Cu²⁺ ions located in the A and B sites; K_{ij} is the exchange parameter between nearest-neighbors Cu²⁺ ions on the octahedral sublattice and H the external magnetic field. The components of the exchange interactions $J_{ij}^{\alpha\alpha}$ are distributed randomly with the same probability, namely

$$\begin{aligned} P(J_{ij}^{xx}, J_{ij}^{yy}, J_{ij}^{zz}) = & 1/3\delta(J_{ij}^{xx} - J_0 - \Delta J)\delta(J_{ij}^{yy} - J_0)\delta(J_{ij}^{zz} - J_0) + \\ & 1/3\delta(J_{ij}^{xx} - J_0)\delta(J_{ij}^{yy} - J_0 - \Delta J)\delta(J_{ij}^{zz} - J_0) + \\ & 1/3\delta(J_{ij}^{xx} - J_0)\delta(J_{ij}^{yy} - J_0)\delta(J_{ij}^{zz} - J_0 - \Delta J), \end{aligned} \quad (12)$$

where $\delta(x)$ is the δ -function. The random numbers P_i^t and P_j^0 determine the distribution \mathbf{P} of the Cu²⁺ ions among the tetrahedral and octahedral sites in the spinel lattice, respectively, so that

$$\mathbf{P}(P_i^{t,0}) = \nu^{t,0}\delta(P_i^{t,0} - 1) + (1 - \nu^{t,0})\delta(P_i^{t,0}) \quad (13)$$

with $\nu^t = 0.25$ and $\nu^0 = 0.75$. The Monte-Carlo simulations were carried out using periodic boundary conditions for a lattice consisting of $24 \times 24 \times 24$ sites and over 30000-60000 MK steps per spins. We calculated the magnetization of the spin lattice, the magnetic susceptibility, and the spin-spin correlation function $\langle S(0)S(R) \rangle$. We simulated the temperature dependence of the EA-order parameter $q(T)$ for the A- and B-spins, respectively, defined as

$$q^{\alpha\beta} = (1/N) \sum_{i=1} \langle S_i^\alpha \rangle^2, \alpha = x, y, z, \beta = t, 0. \quad (14)$$

The exchange parameters ΔJ , K and J_0 were obtained by fitting the MK results to the experimental freezing

temperature T_f , the paramagnetic Néel temperature Θ and the magnetic field dependence of the magnetization $M(H)$. Fig. 15 shows the temperature dependence of the magnetic susceptibility calculated by the Monte-Carlo method for two values of magnetic fields, $H=0$ Oe and $H=10^4$ Oe, respectively. In agreement with the experimental results, the calculated magnetic susceptibility exhibits a cusp at $T_f \simeq 2.5$ K which is suppressed when a magnetic field is applied. As shown in Fig.16 the EA-order parameters for both the A- and B-sublattice sharply increase below $T=T_f$. Moreover, the spin-spin correlation function $\langle S(0)S(L/2) \rangle$ (L =Monte-Carlo sample size) reveals the absence of any long-range magnetic ordering in the spin system. The Monte-Carlo results show that for the concentrations of Cu^{2+} spins of relevance for CuGa_2O_4 , the crystal is in a superparamagnetic state when $K=0$. Introducing random anisotropy for the exchange interaction J results in a spin cluster blocking at the freezing temperature T_f . In that respect, we note that the freezing temperature is proportional to ΔJ . To reproduce the magnetization data in a satisfactory way, we found necessary to give a non-zero value to the antiferromagnetic exchange interaction K . From a least-square refinement of the field dependence of the magnetization we obtained the parameter values $\Delta J/J_0=0.1$, $K/J_0=0.5$. The exchange parameter J_0 , as determined from the freezing temperature T_f , from the paramagnetic susceptibility in the temperature range $90\text{K} \leq T \leq 160\text{K}$ and from the magnetization curve, amounts to -12K, -12.5K and -13 K, respectively. Therefore, the mean values of the model parameters are $J=-12.5\text{K}$, $\Delta J=-1.3\text{K}$, and $K=-6.2\text{K}$.

VII. CONCLUSION

We have presented magnetization, magnetic susceptibility, specific heat and μ SR measurements in CuGa_2O_4 . The data are consistent with a spin-glass transition of the copper sublattice below T_f in this material. In particular, we observe a cusp in the temperature dependence of the magnetic susceptibility at $T_f \simeq 2.5$ K which is suppressed when a magnetic field is applied. A pronounced hysteresis is observed in the temperature dependence of the magnetic susceptibility for zero-field and field-cooled samples. The muon-spin relaxation measurements have shown that above the freezing temperature, the asymmetry function is described by the stretched exponential typical of disordered systems. However, the value of the exponent β points to a narrow distribution of correlation times of the local moments. The temperature dependence of the magnetic volume fraction indicates that in CuGa_2O_4 the transition to a spin-glass state begins around $T \simeq 3.8$ K to form locally clusters of frozen spins which grow when the temperature is lowered and finally percolate around $T_f \simeq 2.5$ K. By means of Monte-Carlo simulations we were able to reproduce the main features

of the magnetic susceptibility and of the magnetization curve measured in CuGa_2O_4 . The results of Monte-Carlo simulations show that the Jahn-Teller effect plays an essential role in forming the magnetic ground-state as it introduces random anisotropy in the exchange interactions between the copper ions, which in turn is responsible for the formation of a spin-glass state in CuGa_2O_4 . Using a realistic spin model which takes into account the effective distribution of the Cu^{2+} ions in the spinel structure, reliable exchange parameters could be obtained for CuGa_2O_4 .

VIII. ACKNOWLEDGMENTS

The work is partially supported by INTAS-97-0177 grant and by CICYT Project 99/142.

- ¹ K.H. Fisher and J.A. Hertz in *Spin Glasses*, Cambridge Studies in Magnetism (1999).
- ² K.H. Fisher, Phys. Stat. Sol. **16**, 357 (1983).
- ³ J. Souletie, J. Physique 39, C2-3 (1978).
- ⁴ M.A. Ruderman and C. Kittel, Phy. Rev. **96**, 99 (1954); T. Kasuya, Prog. Theor. Phys **16**, 45 (1956); K. Yosida, Phys. Rev. **106**, 893 (1957).
- ⁵ H.G. Bohn, W. Zinn, B. Dorner and A. Kollmar, Phys. Rev. B **22**, 5447 (1980).
- ⁶ H. Maletta and P. Convert, Phys. Rev. Lett. **42**, 108 (1979).
- ⁷ S.F. Edwards and P.W. Anderson, J. Phys. F: Metal Phys. **5**, 965 (1975).
- ⁸ L. de Seze, J. Phys. C: Solid State Phys. **10**, L353 (1977).
- ⁹ J. Villain, Z. Physik B **33**, 31 (1979).
- ¹⁰ M. Sparks in *Ferromagnetic Relaxation Theory*, McGraw Hill, 1964.
- ¹¹ P.W. Anderson, Phys. Rev. **102**, 1008 (1956).
- ¹² C.P. Pool Jr., and H.A. Farach, Z. Physik B **47**, 55 (1982).
- ¹³ D. Fiorani, S. Viticoli, J.L. Dormann, J.L. Tholence, and A.P. Murani, Phys. Rev. B **30**, 2776 (1984).
- ¹⁴ Z. Popovic, and S. Satpathy, Phys. Rev. Lett. **84**, 1603 (2000).
- ¹⁵ Guo-meng Zhao, K. Conder, H. Keller, and K.A. Müller, Nature (London) **381**, 676 (1996).
- ¹⁶ A. Shengelaya, Guo-meng Zhao, C.M. Aegerter, K. Conder, I.M. Savić, and H. Keller, Phys. Rev. Lett. **24**, 5142 (1999).
- ¹⁷ K. Kugel and D. Khomsky, Sov. Phys. Usp. **25**, 231 (1982).
- ¹⁸ J.M.R. Gonzales and C.O. Arena, J. Chem. Soc. **1985**, 2155 (1985).
- ¹⁹ W.E. Fogle, J.D. Boyer, R.A. Fisher, and N.E. Phillips, Phys. Rev. Lett. **50**, 1815 (1983).
- ²⁰ S. Kirkpatrick, Phys. Rev. Lett. **36**, 69 (1976).
- ²¹ J.A. Mydosh, *Spin Glasses: An Experimental Introduction*, Taylor and Francis, 1993.
- ²² G. Toulouse and S. Kirkpatrick, J. Phys. (Paris) Lett. **42**, L103 (1981).

²³ K. Emmerich, E. Lippelt, R. Neuhaus, H. Pinkvos, Ch. Schwink, F.N. Gygax, A. Hintermann, A. Schenck, W. Studer and A.J. van der Wal, Phys. Rev. B **31**, 7226 (1985).

²⁴ I.A. Campbell, A. Amato, F.N. Gygax, D. Herlach, A. Schenck, R. Cywinski and S.H. Kylcoyne, Phys. Rev. Lett. **72**, 1291 (1994); A. Kerren, P. Mendels, I. A. Campbell and J. Lord, Phys. Rev. Lett. **77**, 1386 (1996).

²⁵ J.R. Stewart and R. Cywinski, Phys. Rev. B **59**, 4304 (1999) and references therein.

²⁶ R. Kubo, Hyperfine Interact. **8**, 731 (1981).

²⁷ Y.J. Uemura, T. Yamazaki, D.R. Harshman, M. Senba, and E.J. Ansaldo, Phys. Rev. B **31**, 546 (1985).

*On leave of absence in the Kamerlingh Onnes Laboratorium, Leiden University, The Netherlands.

FIG. 1. (a) Real and (b) imaginary parts of the magnetic susceptibility in a single crystal of CuGa₂O₄ as measured with a SQUID magnetometer at a frequency of 19 Hz and in an applied magnetic field of 4.5 Oe.

FIG. 2. Experimental value of the magnetic moment in CuGa₂O₄ for a sample cooled in an applied magnetic field of H=100 Oe (FC curve) and in zero-field (ZFC curve).

FIG. 3. Temperature dependence of the magnetic susceptibility for different magnetic fields.

FIG. 4. Curve 1 shows the magnetic field dependence of the magnetic moment in CuGa₂O₄ at the temperature of T=1.8 K. The magnetic field is applied along the [001] crystal axis. In curve 2, we show the result of the Monte-Carlo simulation for the same field dependence.

FIG. 5. Magnetic susceptibility measured in CuGa₂O₄ for different frequencies.

FIG. 6. Specific heat of CuGa₂O₄.

FIG. 7. Temperature dependence of M/H in CuGa₂O₄ at T=1.8 K.

FIG. 8. Experimental and theoretical dependences of the freezing temperature T_f as a function of the reduced magnetic field h, as explained in the text.

FIG. 9. Experimental zero-field μ SR signal measured in CuGa₂O₄ at T = 10 K, T = 4.5 K and T = 650 mK. The lines represent fits as explained in the text.

FIG. 10. Temperature dependence of the depolarisation rate λ above 3.8 K.

FIG. 11. μ SR spectra measured in CuGa₂O₄ at T = 5 K and showing the field dependence of the asymmetry function. Whereas in zero-field the depolarization function is best described according to Eq. 7, the data with applied field are only fitted by the stretched exponential term reflecting the depolarisation arising from the fluctuating electronic spins (see text).

FIG. 12. Temperature dependence of the parameter A_{magn} corresponding to the magnetic volume fraction.

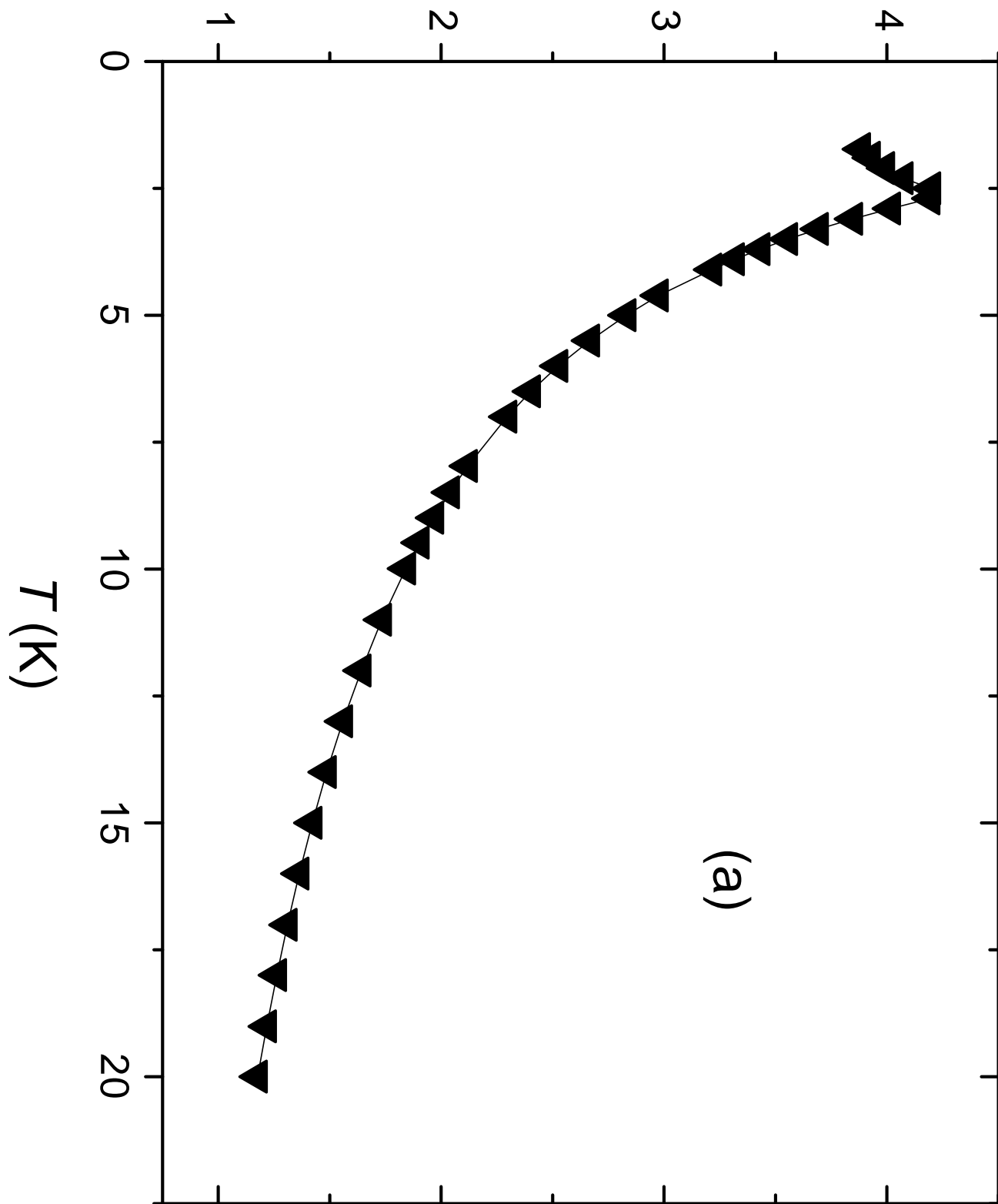
FIG. 13. Temperature dependence of the Δ -parameter of the DKT function. This parameter mirrors the width of the quasi-static field distribution below T_f and therefore the value of the quasi-static Cu²⁺ moment.

FIG. 14. Fit to a μ SR spectrum using the Uemura's function²⁷ (see also text). For sake of clarity the error bars are omitted. The shortcomings of the fit are evident.

FIG. 15. Temperature dependence of the normalized magnetic susceptibility for values of magnetic fields H=0 Oe and H=10⁴ Oe (curve 1 and 2, respectively) with exchange constants J=-12 K, K=-6 K and Δ J=-1.2 K.

FIG. 16. Temperature dependence of the Edwards-Anderson parameter q(T) for the A- and B-sublattice as simulated with Monte-Carlo. See text for details.

$$\chi' (\times 10^{-2} \text{ emu / mol})$$



$$\chi'' \left(\times 10^{-4} \text{ emu / mol} \right)$$

